



Citation for published version:

Jeffrey, MR & Hogan, SJ 2011, 'The geometry of generic sliding bifurcations', *Siam Review*, vol. 53, no. 3, pp. 505-525. <https://doi.org/10.1137/090764608>

DOI:

[10.1137/090764608](https://doi.org/10.1137/090764608)

Publication date:

2011

[Link to publication](#)

©SIAM

University of Bath

Alternative formats

If you require this document in an alternative format, please contact:
openaccess@bath.ac.uk

General rights

Copyright and moral rights for the publications made accessible in the public portal are retained by the authors and/or other copyright owners and it is a condition of accessing publications that users recognise and abide by the legal requirements associated with these rights.

Take down policy

If you believe that this document breaches copyright please contact us providing details, and we will remove access to the work immediately and investigate your claim.

The Geometry of Generic Sliding Bifurcations*

M. R. Jeffrey[†]
S. J. Hogan[†]

Abstract. Using the singularity theory of scalar functions, we derive a classification of sliding bifurcations in piecewise-smooth flows. These are global bifurcations which occur when distinguished orbits become tangent to surfaces of discontinuity, called switching manifolds. The key idea of the paper is to attribute sliding bifurcations to singularities in the manifold's projection along the flow, namely, to points where the projection contains folds, cusps, and two-folds (saddles and bowls). From the possible local configurations of orbits we obtain sliding bifurcations. In this way we derive a complete classification of generic one-parameter sliding bifurcations at a smooth codimension one switching manifold in n dimensions for $n \geq 3$. We uncover previously unknown sliding bifurcations, all of which are catastrophic in nature. We also describe how the method can be extended to sliding bifurcations of codimension two or higher.

Key words. sliding, Filippov, discontinuity, bifurcation, singularity, grazing

AMS subject classifications. 34C23, 37G05, 37G10, 37G15

DOI. 10.1137/090764608

1. Introduction. Bifurcation theory for systems of ordinary differential equations describes how smooth variations of parameter values can, through topological changes, cause sudden changes in dynamics. This paper considers the effect of discontinuous variation in the differential equations themselves, which give rise to the discontinuity-induced bifurcations [6] of piecewise-smooth dynamical systems.

We will study bifurcations that affect individual orbits as a single parameter varies. The flowbox theorem [23] shows that in the neighborhood \mathcal{U} of a point where a flow is smooth and nonvanishing, all orbits are smoothly equivalent. We cannot, therefore, study the global bifurcation of a distinguished orbit Γ passing through \mathcal{U} by studying dynamics in \mathcal{U} alone. The same is not true if the flow is piecewise-smooth in \mathcal{U} with a discontinuity along a surface Σ . Then parameter variation can lead to local changes in the intersection between Γ and Σ . If the change involves orbits which are confined to “sliding” along the discontinuity, then this is called a *sliding bifurcation*. Provided that the discontinuity occurs along a smooth codimension one *switching manifold*, we will show that all one-parameter sliding bifurcations in \mathbb{R}^n are equivalent to just eight cases, each of which occurs generically in \mathbb{R}^2 or \mathbb{R}^3 , and of which only four are already known.

Piecewise-smooth systems are widespread in applications such as engineering, economics, medicine, biology, and ecology. Problems with impacts, friction, or switching

*Received by the editors July 13, 2009; accepted for publication (in revised form) August 31, 2010; published electronically August 5, 2011. This work was supported by EPSRC grant EP/E032249/1. <http://www.siam.org/journals/sirev/53-3/76460.html>

[†]Bristol Centre for Applied Nonlinear Mathematics, Department of Engineering Mathematics, University of Bristol, Bristol, BS8 1TR, UK (mike.jeffrey@bristol.ac.uk).

are piecewise-smooth. For recent accounts of such systems, see [6, 21, 34]. The systems we consider are expressible in the form

$$(1.1) \quad \dot{x} = f(x, t; \mu),$$

where $x \in \mathbb{R}^n$ is a state vector, $\mu \in \mathbb{R}$ is a parameter (which may more generally be a vector), and $\dot{x} = dx/dt$ with $t \in \mathbb{R}$. The function $f : \mathbb{R}^{n+2} \rightarrow \mathbb{R}^n$ is piecewise-smooth, with discontinuities occurring across a hypersurface through phase space, called the switching manifold.

To fully define solutions of (1.1), a rule must be given to prescribe the dynamics at the switching manifold. If the rule is to apply a map from one point on the manifold to another, the solution $x(t)$ can be discontinuous, leading to hybrid or impact systems [6]. The subject of this paper is systems where the solution $x(t)$ remains continuous, but can be nonunique at the manifold [10]. A local form for such systems is

$$(1.2) \quad \dot{x} = f(x; \mu) = \begin{cases} f^+(x; \mu) & \text{if } h(x) > 0, \\ f^-(x; \mu) & \text{if } h(x) < 0, \end{cases}$$

where $h(x) = 0$ implicitly defines the switching manifold. Each of the vector fields f^+ and f^- is smooth and defined for all x . At $h = 0$, trajectories either cross through the switching manifold or slide along it; see Figure 1.1.

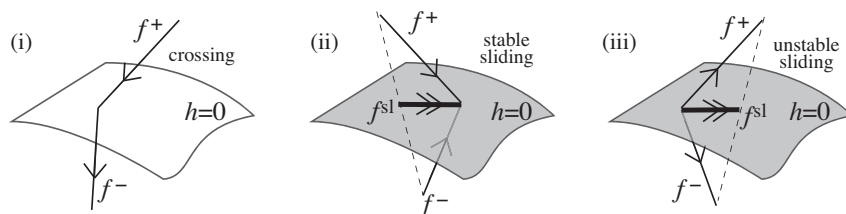


Fig. 1.1 Piecewise-smooth vector fields in regions of (i) crossing, (ii) stable sliding, and (iii) unstable sliding. The sliding vector field f^{sl} (double arrows) is a convex combination of f^+ and f^- . This formalism is due to Filippov [10] and Utkin [32] and is said to define a Filippov system.

Sliding trajectories are solutions of

$$(1.3) \quad \dot{x} = f^{\text{sl}} \equiv (1 - \lambda)f^+ + \lambda f^-, \quad \text{where} \quad \lambda = \frac{\mathcal{L}_{f^+} h}{(\mathcal{L}_{f^+} h - \mathcal{L}_{f^-} h)},$$

defined on $h = 0$ wherever $(\mathcal{L}_{f^+} h)(\mathcal{L}_{f^-} h) < 0$, where \mathcal{L}_f denotes the Lie derivative $\mathcal{L}_f \equiv f \cdot \frac{d}{dx}$ along the flow of f and $\frac{d}{dx}$ is the gradient. (Later we will also make use of the n -th derivative $\mathcal{L}_f^n \equiv (\mathcal{L}_f)^n$.) The sliding vector field f^{sl} is a convex combination of f^+ and f^- , with λ defined such that f^{sl} is always tangent to the manifold.

DEFINITION 1.1. An orbit segment is a smooth curve which is a trajectory of (1.2) in the regions $h > 0$ or $h < 0$. A sliding segment is a smooth curve which is a trajectory of (1.3) on $h = 0$. An orbit is a continuous curve $x(t)$ that is a concatenation of orbit segments and sliding segments.

DEFINITION 1.2. A topological equivalence between Filippov systems $F = \{f, f^{\text{sl}}\}$ and $F' = \{f', f'^{\text{sl}}\}$ is a homeomorphism on \mathbb{R}^n that sends orbits of F to orbits of F' , preserving orbit segments, sliding segments, and time direction.

For more detailed definitions, see [10, 20]. Note this is stronger than a definition given in [1] because orbits, not just segments, are preserved. This is essential in the present paper, as it respects the intersection of orbits with the switching manifold.

Orbits are then continuous, but need not be differentiable (following Filippov's convention [10]). Where $\lambda < 0$ or $\lambda > 1$ in (1.3), we have $(\mathcal{L}_{f^+}h)(\mathcal{L}_{f^-}h) > 0$; then orbit segments either side of $h = 0$ can be concatenated to form an orbit that crosses the switching manifold (see Figure 1.1(i)).

Orbit segments can also be concatenated with sliding segments. Orbits with sliding segments are nonunique in the sense that infinitely many orbits pass through any point in the sliding region. Sliding regions on $h = 0$ satisfy $0 < \lambda < 1$ and come in two forms. If $\mathcal{L}_{f^+}h < 0 < \mathcal{L}_{f^-}h$, then the sliding is *stable* (see Figure 1.1(ii)): orbits reach the manifold in finite time and follow the sliding vector field f^{sl} along it. If $\mathcal{L}_{f^+}h > 0 > \mathcal{L}_{f^-}h$, then the sliding is *unstable* (see Figure 1.1(iii)): orbits follow the sliding vector field on the switching manifold, but also escape into $h > 0$ and $h < 0$. The stability type can be interchanged by reversing the arrow of time. Unstable sliding, sometimes called “escaping,” has historically received less attention, but will play a vital role in what follows.

Boundaries between sliding and crossing occur where $\mathcal{L}_{f^+}h$ or $\mathcal{L}_{f^-}h$ vanish, implying that f^+ or f^- in (1.2) are tangent to the switching manifold. Since $\mathcal{L}_{f^+}h = 0 \Rightarrow \lambda = 0$ and $\mathcal{L}_{f^-}h = 0 \Rightarrow \lambda = 1$, from (1.3) we have the following boundary conditions for f^{sl} :

$$(1.4) \quad \begin{cases} f^{\text{sl}} = f^+ & \text{if } \mathcal{L}_{f^+}h = 0, \\ f^{\text{sl}} = f^- & \text{if } \mathcal{L}_{f^-}h = 0. \end{cases}$$

A tangency is called *visible* or *invisible* depending on whether orbits locally curve away from, or toward, the manifold, as illustrated in Figures 1.2(i)–(ii). It is also possible for sliding segments to be tangent to the sliding region's boundary, and these similarly are referred to as either visible or invisible, as shown in Figures 1.2(iii)–(iv). When a tangency occurs in the vector field, we say that an orbit there is *grazing*.

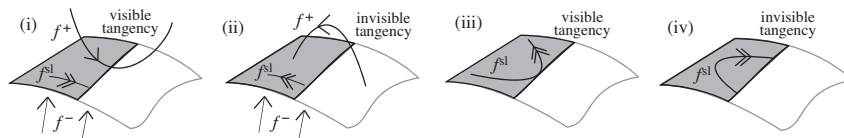


Fig. 1.2 Tangencies in a piecewise-smooth system. Visible (i) and invisible (ii) tangencies form the boundaries between sliding (shaded) and crossing (unshaded). Tangencies between the sliding vector field and the sliding region's boundary can also be visible (iii) or invisible (iv).

Hence, a grazing orbit is a nongeneric trajectory which, under perturbation, loses or gains points of intersection with the manifold. This leads to the observation that orbits in Filippov systems can undergo a variety of topological changes, called *sliding bifurcations*. Originally proposed in the Russian literature [9], until recently only the cases sketched in Figure 1.3 were known [20]. The aim of this paper is to give a systematic classification of sliding bifurcations, and this will reveal hitherto unknown cases where unstable sliding plays a vital role.

We will now define sliding bifurcations and introduce the central result of the paper, Theorem 1.4. The different sliding bifurcations will be described in section 5.

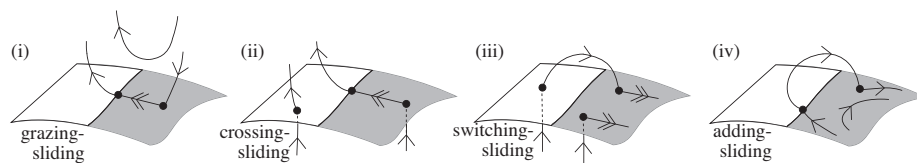


Fig. 1.3 Four sliding bifurcations: (i) grazing-sliding, (ii) crossing-sliding, (iii) switching-sliding, and (iv) adding-sliding [6]. In each case the sliding region (shaded) is stable. These have been found, for example, in relay circuits, dry-friction oscillators, and predator-prey models [6, 7, 8, 20].

A bifurcation occurs in a system if an arbitrarily small perturbation gives topologically nonequivalent orbits according to Definition 1.2. If topological equivalence is lost due to a change in a particular orbit's intersection with the switching manifold, we say it undergoes a sliding bifurcation, defined as follows.

DEFINITION 1.3. A distinguished orbit $x(t; \mu)$ of (1.2)–(1.3) undergoes a sliding bifurcation at $x = \mu = 0$ if the vector field $f^+(0; 0)$ or $f^-(0; 0)$ is tangent to the switching manifold, and an arbitrarily small perturbation in μ gives a topologically nonequivalent orbit. We will refer to the μ -family of orbits as an unfolding of the sliding bifurcation.

There are three types of tangency that will feature in this paper. The simplest is a quadratic contact between the vector field and the manifold, as in Figures 1.2(i)–(ii), called a *fold*. The next is a cubic contact, called a *cusp*, which is responsible for the sliding tangencies shown in Figures 1.2(iii)–(iv). The third is a quadratic contact to both sides of the manifold, called a *two-fold*. We need not consider any higher-order tangencies because of the following theorem, which we prove in section 5.7.

THEOREM 1.4. A generic one-parameter sliding bifurcation in \mathbb{R}^n for any $n \geq 3$ occurs at either a fold, cusp, or two-fold.

The rest of this paper is organized as follows. We conclude the present section with a brief discussion of what is meant by the term “sliding bifurcation.” In section 2, we properly define the tangencies that occur generically in Filippov systems in \mathbb{R}^2 and \mathbb{R}^3 . In section 3, we give an explicit local form for Filippov systems as straight vector fields either side of a curved switching manifold. This leads to the key idea of the paper, in section 4, to derive normal forms for the manifold from singularity theory [2, 3, 11], and then to add dynamics to derive sliding bifurcations in each setting. This is an alternative to previous uses of singularity theory in nonsmooth systems, where normal forms were derived for divergent diagrams [22, 28] and for vector fields tangent to a switching manifold [30] or to a boundary [26, 33].

The main results of the paper follow in section 5, where we first derive an unfolding around nongeneric trajectories and then use it to find a complete classification of one-parameter sliding bifurcations. In section 5.7, we show that these form the building blocks for all one-parameter sliding bifurcations in \mathbb{R}^n , and some codimension two sliding bifurcations are described in section 5.8. In the appendix we show that our geometric approach reproduces the normal forms for vector fields at flat switching manifolds, which are equivalent to those provided by other authors, and thus applies to generic Filippov systems.

1.1. What Is a Sliding Bifurcation? A key insight behind Theorem 1.4 is that the topological instability constituting a sliding bifurcation is localized to the neigh-

borhood of the switching manifold [8]. Consider a distinguished orbit entering the neighborhood \mathcal{U} of a point on the switching manifold. The orbit is distinguished by global conditions, but the changes it can undergo relative to the manifold, in \mathcal{U} , depend only on the configurations of orbits that are possible in \mathcal{U} . As the orbit explores these different configurations it undergoes sliding bifurcations, and the same bifurcations therefore affect, for example, (i) an unstable manifold and (ii) a periodic orbit, as shown in Figure 1.4. Thus, sliding bifurcations are *local* mechanisms for *global* bifurcations.

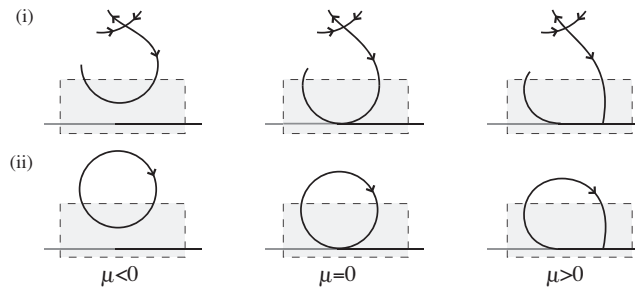


Fig. 1.4 Sliding bifurcations as a local mechanism for global bifurcations. As μ changes a sliding segment is created in (i) the stable manifold to a saddle and (ii) a periodic orbit. The topological change is the same: locally (gray box) the phase portraits for (i) and (ii) are equivalent.

One way of describing this is to let $x(t; \mu)$ denote, for each $\mu > 0$, an orbit of (1.2)–(1.3) that is an organizing center of the global dynamics. Let this graze at $x = 0$ when $\mu = 0$. Define a map $T_\mu : \mathbb{R}^n \mapsto \mathbb{R}^n$ that induces a map on the vector fields $f(x; \mu)$ and $f^{\text{sl}}(x; \mu)$, given in the neighborhood of $x = 0$ by

$$(1.5) \quad T_\mu(f(x; 0), f^{\text{sl}}(x; 0)) = \{f(x; \mu), f^{\text{sl}}(x; \mu)\}.$$

Assume that T_μ does not induce any bifurcation of f^+ or f^- . Nevertheless, typically the orbit $x(t; \mu)$ is no longer grazing for $\mu \neq 0$ and thus has undergone a sliding bifurcation by Definition 1.3. If we now apply the inverse map T_μ^{-1} to the vector field, it returns locally to the form $\{f(x; 0), f^{\text{sl}}(x; 0)\}$, but the orbit $x(t; \mu)$ is defined globally, so it will map to some new orbit whose local expression is $\tilde{x}(t; \mu)$ and satisfies $\tilde{x}(t; 0) = x(t; 0)$. The sliding bifurcation then unfolds *locally* as a μ -family of orbits $\tilde{x}(t; \mu)$ in the unchanging vector field given by $\{f(x; 0), f^{\text{sl}}(x; 0)\}$. We will use such μ -families in an unchanging vector field to unfold the sliding bifurcations in section 5.

2. Singularities and the Vector Field. In this section, we introduce the tangencies of piecewise-smooth vector fields that are generic in \mathbb{R}^3 , as proven in [30]. Because we are interested only in tangencies between the vector field and the manifold, let us assume that f^+ and f^- are linearly independent throughout the local region of interest. This implies that $f^\pm \neq 0$ and, from (1.3), that $f^{\text{sl}} \neq 0$.

The simplest tangency is a quadratic contact between the switching manifold and *one* of the vector fields f^\pm . Without loss of generality let us choose a tangency with f^+ , which occurs where $\mathcal{L}_{f^+}h = 0$, which is quadratic if $\mathcal{L}_{f^+}^2h \neq 0$. Depending on the sign of $\mathcal{L}_{f^+}h$ the tangency is visible or invisible (see Figures 1.2(i)–(ii)), and since f^- is not tangent to $h = 0$ we have $\mathcal{L}_{f^-}h \neq 0$. We call a point where these conditions are satisfied a *fold*. It is generic in \mathbb{R}^n for $n \geq 2$ and defined as follows.

DEFINITION 2.1. *At a fold, $\mathcal{L}_{f+}h = 0$, $\mathcal{L}_{f+}^2h \neq 0$, $\mathcal{L}_{f-}h \neq 0$, and the fold is*

1. *visible if $\mathcal{L}_{f+}^2h > 0$,*
2. *invisible if $\mathcal{L}_{f+}^2h < 0$.*

The contact between the vector field and the manifold is cubic if \mathcal{L}_{f+}^2h also vanishes and $\mathcal{L}_{f+}^3h \neq 0$. Then f^+ and, by (1.4), f^{sl} are tangent to the set of fold points where $\mathcal{L}_{f+}h = 0$. The signs of \mathcal{L}_{f+}^3h and $\mathcal{L}_{f-}h$ determine whether the tangency of f^{sl} is visible or invisible (see Figures 1.2(iii)–(iv)). We call a point where these conditions are satisfied a *cusp*, defined as follows.

DEFINITION 2.2. *At a cusp, $\mathcal{L}_{f+}h = \mathcal{L}_{f+}^2h = 0$, $\mathcal{L}_{f+}^3h \neq 0$, $\mathcal{L}_{f-}h \neq 0$, and the vectors $\frac{d}{dx}h$, $\frac{d}{dx}\mathcal{L}_{f+}h$, $\frac{d}{dx}\mathcal{L}_{f+}^2h$ are linearly independent. The cusp is*

1. *visible if $(\mathcal{L}_{f+}^3h)(\mathcal{L}_{f-}h) < 0$,*
2. *invisible if $(\mathcal{L}_{f+}^3h)(\mathcal{L}_{f-}h) > 0$.*

The fold and cusp lie on the boundary of stable sliding if $\mathcal{L}_{f-}h > 0$ and of unstable sliding if $\mathcal{L}_{f-}h < 0$ (recall Figure 1.1 for the types of stability). If a quadratic contact occurs between the manifold and *both* of the vector fields f^+ and f^- at the same point, then $\mathcal{L}_{f+}h = \mathcal{L}_{f-}h = 0$, but the second derivatives are nonzero. Thus, we have a fold with respect to both f^+ and f^- , each of which may be visible or invisible, and we call such a point a *two-fold*, defined as follows.

DEFINITION 2.3. *At a two-fold, $\mathcal{L}_{f+}h = \mathcal{L}_{f-}h = 0$, $\mathcal{L}_{f\pm}^2h \neq 0$, and the vectors $\frac{d}{dx}h$, $\frac{d}{dx}\mathcal{L}_{f+}h$, $\frac{d}{dx}\mathcal{L}_{f-}h$ are linearly independent. The two-fold is*

1. *visible if $\mathcal{L}_{f+}h > 0$ and $\mathcal{L}_{f-}h < 0$,*
2. *invisible if $\mathcal{L}_{f+}h < 0$ and $\mathcal{L}_{f-}h > 0$,*
3. *visible-invisible if $(\mathcal{L}_{f+}h)(\mathcal{L}_{f-}h) > 0$.*

Given Theorem 1.4, the conditions in Definitions 2.1–2.3 are necessary and sufficient for the existence of one-parameter sliding bifurcations. To find what those bifurcations look like, we will begin by finding an explicit local approximation for the piecewise-smooth system.

3. Local Piecewise-Straightening. Having fixed f^+ and f^- to be linearly independent, let us now consider them to lie along the axes of a coordinate system $x = (x_1, x_2, x_3)$ in \mathbb{R}^3 , so that the vector field in (1.2) becomes simply

$$(3.1) \quad \dot{x} = f(x) = \begin{cases} f^+ = (1, 0, 0) & \text{if } h(x) > 0, \\ f^- = (0, 1, 0) & \text{if } h(x) < 0, \end{cases}$$

hence its Lie derivative is given by $\mathcal{L}_f = \mathcal{L}_{f+} \equiv \frac{\partial}{\partial x_1}$ for $h > 0$ and $\mathcal{L}_f = \mathcal{L}_{f-} \equiv \frac{\partial}{\partial x_2}$ for $h < 0$. We can reverse time in $h > 0$ or $h < 0$ by changing the signs of f^+ or f^- . We can also extend this to \mathbb{R}^n for $n > 3$ by adding zeros beyond the third component.

It remains to derive typical forms of h in such a system. Letting the switching manifold $h = 0$ be a general curved surface, we will relate tangencies in the system to the manifold's geometry. Moreover, in the appendix we show that previous authors' normal forms for piecewise-smooth vector fields with folds, cusps, or two-folds [10, 20, 30] are equivalent to (3.1) with appropriate forms of h which we find in section 4.

Let us now consider the form of the switching manifold. If there is a fold or cusp at $x = 0$ in (3.1), then, applying the Lie derivatives for (3.1) to Definitions 2.1–2.2, we have $\partial h(0)/\partial x_2 \neq 0$. Then we can find coordinates $x = (x_1, x_2, x_3)$, where

$h(x) = x_2 + V(x)$, given $\partial V(0)/\partial x_2 = 0$. To lowest order in x_2 (for small x),

$$(3.2) \quad h(x_1, x_2, x_3) = x_2 + V(x_1, x_3).$$

If instead there is a two-fold at $x = 0$, then applying the Lie derivatives for (3.1) to Definition 2.3 shows that the coordinate axes x_1 and x_2 lie in the tangent plane of the switching manifold. Thus, the only nonvanishing first derivative of h is $\partial h/\partial x_3 \neq 0$, and to lowest order in x_3 (for small x) we can write

$$(3.3) \quad h(x_1, x_2, x_3) = x_3 + V(x_1, x_2),$$

where $\partial V(0)/\partial x_3 = 0$. In the following section we will use results from singularity theory to find local expressions for the function V .

4. Singularity Theory and the Switching Manifold. We now introduce some standard results of singularity theory applied to smooth surfaces. We cover only the ideas required for this paper and refer the reader to [2, 3, 11] for particularly readable accounts of the precise statements and theory behind them.

A scalar-valued function $V(u, a)$ of a variable $u \in \mathbb{R}^p$ and a parameter $a \in \mathbb{R}^q$ can be characterized by locally classifying its stationary points where the gradient dV/du vanishes. For a function V with a nondegenerate stationary point at $u = 0$, the Morse lemma [24] states that we can find local coordinates $u = (u_1, u_2, \dots, u_n)$ in which $V(u, a) = V(u) = \pm \frac{1}{2}u_1^2 \pm \frac{1}{2}u_2^2 \cdots \pm \frac{1}{2}u_n^2$. The set $h = 0$ of a function $h(u, v) = v + V(u)$, for $v \in \mathbb{R}$, then has a fold singularity in the space of (u, v) when projected along any of the coordinate axes of u . The zero set of h with a fold along u_1 is illustrated in Figure 4.1(i), plotted in coordinates $(x_1, x_2) = (u_1, v)$. Folds along u_1 and u_2 are illustrated in Figures 4.1(iii)–(iv) in the space $(x_1, x_2, x_3) = (u_1, u_2, v)$.

A stationary point is degenerate if the Hessian determinant vanishes, so $|d^2V/du^2| = dV/du = 0$. At a degenerate stationary point an invertible coordinate transformation can typically be found to express V in a “normal form,” which belongs to a parameterized family of functions called a universal unfolding. The universal unfolding displays the nondegenerate components making up the degeneracy over the space of u , in which, as parameters vary, sets of nondegenerate stationary points emanate from the degeneracies. A universal unfolding is structurally stable, that is, the pattern of stationary points and degeneracies persists under small perturbations to the unfolding.

For a scalar function V with a degenerate stationary point $dV(0)/du = d^2V(0)/du^2 = 0 \neq d^3V(0)/du^3$, we can find a local coordinate $u = u_1$ such that $V(u_1) = \frac{1}{3}u_1^3$. This is structurally unstable. The normal form of its universal unfolding is $V(u_1, a) = \frac{1}{3}u_1^3 + au_1$, where a is a real parameter, so that $\partial^2V(0, 0)/\partial u_1 \partial a \neq 0$ ensures structural stability [24]. For a function $h(u, v, a) = v + V(u, a)$, the level sets of h have curves of fold singularities when projected along the u_1 -coordinate axis in the space of (u_1, v, a) , except at $u_1 = a = 0$, where the projection has a cusp at which two-folds meet. This is illustrated in Figure 4.1(ii) in coordinates $(x_1, x_2, x_3) = (u_1, v, a)$.

In general, the dimension of the parameter a in $V(x, a)$ is the smallest possible for the unfolding to be stable, called the *codimension*. Only the singularities in Figure 4.1 (of codimension 0 or 1) will feature in this paper. We discuss the role of higher codimension singularities in sliding bifurcations in sections 5.7–5.8.

These ideas are of use in dynamical systems if a problem can be reduced to considering a scalar function; for example, in a gradient dynamical system $\dot{u} = dV(u)/du$, an unfolding $V(u_1, a) = \frac{1}{3}u_1^3 + au_1$ would describe a saddle-node bifurcation [19]. The

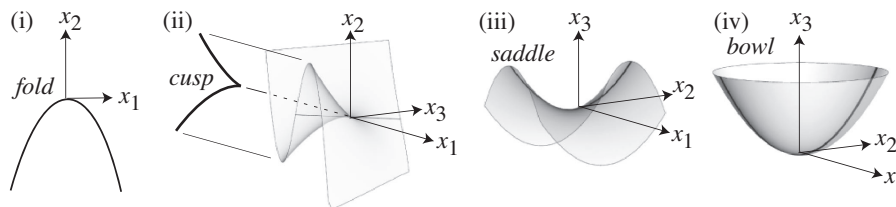


Fig. 4.1 Generic singularities of the function $h = 0$ for (i) the fold $h = x_2 + \frac{1}{2}x_1^2$; (ii) the cusp $h = x_2 + (\frac{1}{3}x_1^3 + x_3x_1)$; the two-fold, which is either (iii) a saddle $h = x_3 + (\frac{1}{2}x_1^2 - \frac{1}{2}x_2^2)$ or (iv) a bowl $h = x_3 + (\frac{1}{2}x_1^2 + \frac{1}{2}x_2^2)$. Writing $h(u, v, a) = v + V(u, a)$, the x -coordinates correspond to (i) $(x_1, x_2) = (u_1, v)$, (ii) $(x_1, x_2, x_3) = (u_1, v, a)$, and (iii)–(iv) $(x_1, x_2, x_3) = (u_1, u_2, v)$.

central idea of the present paper is to exploit (3.2)–(3.3), whereby the switching manifold is expressed as the zero set of a scalar function $h = v + V$. Then, at a fold or cusp, from (3.2), the switching manifold is given by $h(x_1, x_2, x_3) = x_2 + V(x_1, x_3) = 0$. In the straightened vector field of (3.1) there are no dynamics in the x_3 direction, and hence x_3 behaves like a parameter, so we can map (u_1, v) onto the coordinates (x_1, x_2) as in Figure 4.1(i), or map (u_1, v, a) onto the coordinates (x_1, x_2, x_3) as in Figure 4.1(ii). Transformations on the coordinates x_1 only are sufficient to put V into either of the normal forms $V = \pm \frac{1}{2}x_1^2$ or $V = \frac{1}{3}x_1^3 + x_3x_1$, since x_3 can be chosen arbitrarily because $\dot{x}_3 = 0$ in (3.1). It is easily verified, by applying the Lie derivatives for (3.1), that the straightened vector field with

$$(4.1) \quad h(x_1, x_2) = x_2 \pm \frac{1}{2}x_1^2$$

describes a fold in the vector field consistent with Definition 2.1, and with

$$(4.2) \quad h(x_1, x_2, x_3) = x_2 + \frac{1}{3}x_1^3 + x_3x_1$$

describes a cusp in the vector field consistent with Definition 2.2.

At a two-fold, according to (3.3), we can express the switching manifold as $h(x_1, x_2, x_3) = x_3 + V(x_1, x_2) = 0$. If we simply let $(u_1, u_2, v) = (x_1, x_2, x_3)$, then the vector field in (3.1) would lie tangent to the fold curves on $h = 0$ and violate the non-degeneracy conditions in Definition 2.3. Instead, we map a linear combination of u_1 and u_2 to x_1 and x_2 , obtaining a general expression for V as $V = c_1x_1^2 + c_2x_2^2 + c_3x_1x_2$. We are free to choose the constants c_i to give

$$(4.3) \quad h(x_1, x_2, x_3) = x_3 + \frac{1}{2}\alpha x_1^2 - \frac{1}{2}\beta x_2^2 + x_1x_2,$$

where the parameters α and β describe the alignment of the folds to the coordinate axes and must be nonzero. Applying the Lie derivatives for (3.1), it is easily seen that the straightened vector field in (3.1), with V given by (4.3), describes a two-fold consistent with Definition 2.3.

5. Sliding Bifurcations. This section concerns the dynamics implied by the local geometry. We have derived a local expression in which the vector field is straight, (3.1), while the switching manifold is curved and specified by one of (4.1)–(4.3). In this section we will characterize the flow by finding a surface composed of a generic family of orbits. The surface will be expressed implicitly as a function $\psi(x) = 0$ and describes the typical shape of orbits in the piecewise-smooth flow. By considering

how the surfaces $\psi = 0$ and $h = 0$ intersect, we can study how orbits lose or gain points of intersection with the switching manifold near grazing.

In general, if a scalar function $\psi(x)$ in \mathbb{R}^3 satisfies $\mathcal{L}_f\psi(x) = 0$, then a surface defined by $\psi(x) = 0$ consists of a one-parameter family of orbits of a system $\dot{x} = f$, where $f \neq 0$. For (3.1), a suitable scalar function is

$$(5.1) \quad \psi(x) = \rho(x_3) - x_i + h(x) - h(x)g(x) \quad \text{with} \quad g = \frac{\mathcal{L}_f(h - x_i)}{\mathcal{L}_fh},$$

where ρ is a smooth function and g is piecewise-constant (as we show in (5.3) below). The coordinate x_i is the x component preceding V in each of the expressions of the form $h = x_i + V$ given by (4.1)–(4.3). The surface $\psi = 0$ is piecewise-smooth. When $\rho = 0$, it contains an orbit intersecting the origin, and therefore $\psi = 0$ is an unfolding of a sliding bifurcation as defined in Definition 1.3.

The surface $\psi = 0$ is comprised of a family of orbits in each of the vector fields f^+ and f^- , which have a common intersection on $h = 0$. Generically, the portions of $\psi = 0$ in $h > 0$ and $h < 0$ will each be transverse to $h = 0$. This implies that $d\psi/dx$ and dh/dx must be linearly independent. Then the intersection between $\psi = 0$ and the switching manifold $h = 0$ is a smooth curve $x_i = \rho(x_3)$, and hence ρ determines the shape of the surface $\psi = 0$. We parameterize this intersection curve as $x_0(\mu)$ for $\mu \in \mathbb{R}$, and we call points $x = x_0(\mu)$ the *impact coordinates*. They are found by solving

$$(5.2) \quad h(x_0) = 0 \quad \text{and} \quad \psi(x_0) = 0.$$

We will use the impact coordinates x_0 as initial data for orbits in the unfolding.

The piecewise-constant g must be evaluated on each side of the switching manifold. On a given side, if grazing occurs, then $\mathcal{L}_fx_i = 0$ and $g = 1$; otherwise we must have $\mathcal{L}_f(h - x_i) = 0$ over a neighborhood of $x = 0$, giving $g = 0$. Therefore,

$$(5.3) \quad g = \begin{cases} 1 & \text{if } \mathcal{L}_fx_i = 0, \\ 0 & \text{if } \mathcal{L}_f(h - x_i) = 0 \end{cases} \quad \text{at } x = 0.$$

Note that only one of the two is possible on each side of the manifold.

In the remainder of this section we make explicit the unfoldings $\psi = 0$ given by (5.1). In this way we classify and unfold the one-parameter sliding bifurcations that are possible in the neighborhood of the singularities in section 4. The reader may find it useful to also refer to Figure A.1 in the appendix, where we reproduce these results for a flat switching manifold.

5.1. Sliding Bifurcation at a Visible Fold: Grazing Case. Consider the vector field in (3.1) with switching manifold $h(x) = x_2 + \frac{1}{2}x_1^2 = 0$ from (4.1). By result (1) of Definition 2.1, this represents a visible fold. By setting $\rho = x_3$ in (5.1), we obtain an unfolding of the *sliding bifurcation at a visible fold*, given by $\psi = 0$, where

$$(5.4) \quad \begin{aligned} \psi(x) &= x_3 - x_2 + h(x)\Theta[-h(x)] \quad \text{and} \\ h(x) &= x_2 + \frac{1}{2}x_1^2, \end{aligned}$$

where Θ is the unit step function $\Theta[h] = \frac{1}{2}(1 + \text{sgn}[h])$. We have simplified (5.4) using the identity $\Theta[h] = 1 - \Theta[-h]$. This unfolding is shown in Figure 5.1(i). We will now describe this figure, and we remind the reader that the vector field f^- in $h < 0$ is vertical and points toward the switching manifold (for clarity the arrows of f^- are not shown in Figure 5.1(i)). Note that the sliding region is stable because $\mathcal{L}_{f^-}h > 0$.

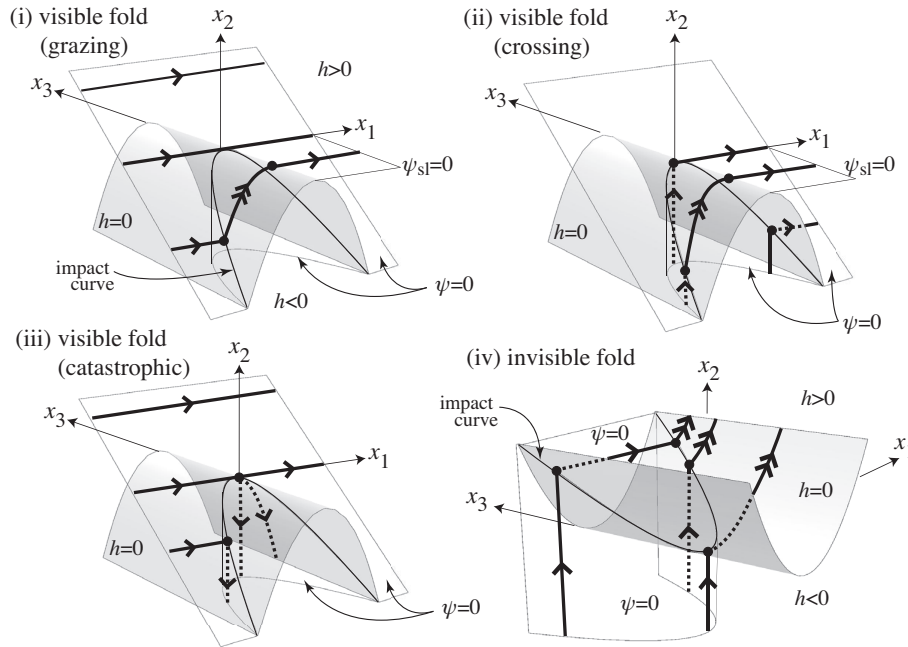


Fig. 5.1 *Sliding bifurcation at a fold. The switching manifold is the shaded surface $h = x_2 \pm \frac{1}{2}x_1^2 = 0$. A nongeneric orbit intersects the origin. Its unfolding is $\psi = 0$, with sliding separatrix $\psi_{sl} = 0$ (in (i)–(ii) only). The sliding bifurcations are classified as (i) at a visible fold (grazing case), where the nongeneric orbit visibly grazes at the boundary of stable sliding; (ii) at a visible fold (crossing case), where the nongeneric orbit crosses the manifold at the boundary of stable sliding; (iii) at a visible fold (catastrophic case), where the nongeneric orbit splits into grazing, crossing, and sliding solutions at the boundary of unstable sliding; (iv) at an invisible fold, where the nongeneric orbit hits the fold transversally. Arrows can be reversed in each case to obtain the same four phase portraits with the opposite stability of sliding.*

Orbits cross the switching surface $h = 0$ where $x_1 > 0$ and slide where $x_1 < 0$. Sliding orbits (double arrows) flow toward the fold (as implied by the conditions in (1.4)), then escape into $h > 0$. The segments of orbits leaving the switching manifold at the fold form a surface given by $\psi_{sl} = 0$, where

$$(5.5) \quad \psi_{sl}(x) = -x_2 + h(x)\Theta[-h(x)], \quad x_1 \geq 0.$$

This is the *sliding separatrix* that separates orbits with sliding dynamics from those with crossing dynamics. The solution of $\psi_{sl} = 0$ is simply $x_2 = 0$ for $h > 0$ (the section of horizontal plane in Figure 5.1(i)) and $x_1 = 0$ for $h < 0$, and is the nongeneric zero level surface of (5.1) with $\rho = 0$, whose intersection with $h = 0$ is the fold.

Using (5.2), we find that impact points in the unfolding satisfy $0 = x_3 + \frac{1}{2}x_1^2$. If we parameterize this curve as $x_0(\mu) = (\pm\sqrt{-2\mu}, \mu, \mu)$, then μ labels a family of orbits originating in $h > 0$. The nongeneric orbit at $\mu = 0$ grazes the manifold; see Figure 5.1(i). This implies a sliding bifurcation: for $\mu > 0$, each orbit is a smooth trajectory in $h > 0$, and for $\mu < 0$, each orbit impacts on the curve $x_0(\mu) = (-\sqrt{-2\mu}, \mu, \mu)$. We call this the *grazing case* of the sliding bifurcation at a visible fold. See also Figure A.1(1), where this is illustrated for a flat switching manifold. It describes, for instance, the grazing-sliding of a limit cycle shown in Figure 1.3(i).

5.2. Sliding Bifurcation at a Visible Fold: Crossing Case. Orbits that originate in $h < 0$ in the unfolding given by (5.4) behave somewhat differently, as shown in Figure 5.1(ii). We can reparameterize the curve of impact coordinates as $x_0(\mu) = (\mu, -\frac{1}{2}\mu^2, -\frac{1}{2}\mu^2)$, and consider the nongeneric orbit at $\mu = 0$. This is transverse to the switching manifold, but it intersects the fold from $h < 0$, implying a different sliding bifurcation to section 5.1. On one side of the bifurcation, $\mu > 0$, the orbit crosses the manifold. On the other side, $\mu < 0$, the orbit has a sliding segment connecting the curve $\{x_0(\mu) : \mu < 0\}$ to the fold, and it escapes the manifold on the sliding separatrix $\psi_{sl} = 0$ given by (5.5). We call this the *crossing case* of the sliding bifurcation at a visible fold. See Figure A.1(2) for its illustration at a flat switching manifold. It describes, for instance, the crossing-sliding of a limit cycle shown in Figure 1.3(ii).

5.3. Sliding Bifurcation at a Visible Fold: Catastrophic Case. If we reverse the time direction for $h < 0$ in the system (3.1), so that $\mathcal{L}_f - h < 0$, and keep the same unfolding from (5.4), then orbits originating in $h > 0$ undergo a discontinuous change as they pass through grazing, as shown in Figure 5.1(iii).

As for the grazing case, in section 5.1, we can label orbits by parameterizing the impact coordinates as $x_0(\mu) = (\pm\sqrt{-2\mu}, \mu, \mu)$. The nongeneric orbit at $\mu = 0$ grazes the manifold. When it grazes, the solution becomes nonunique, since it can remain in $h > 0$ as a smooth orbit, or cross through to $h < 0$, or enter the unstable sliding region; all three possibilities are shown in Figure 5.1(iii).

For $\mu > 0$, the orbit is smooth, lies in $h > 0$, and does not impact the manifold. For $\mu < 0$, the orbit crosses the manifold on the curve $x_0(\mu) = (-\sqrt{-2\mu}, \mu, \mu)$, and the outgoing trajectory crosses to $h < 0$. This is the *catastrophic case* of the sliding bifurcation at a visible fold. The phase portrait is equivalent to neither the grazing nor the crossing cases from sections 5.1–5.2. The sliding bifurcation is catastrophic in the sense that perturbing the grazing orbit causes a discontinuous change in its outset from the neighborhood of the fold, while its inset changes continuously. See Figure A.1(5) for its illustration at a flat switching manifold.

This sliding bifurcation describes, for instance, the catastrophic destruction of a limit cycle by grazing-sliding. As a catastrophic event, it is qualitatively different from the sliding bifurcations in sections 5.1–5.2 and those in sections 5.4–5.5 which follow, yet it arises naturally in our classification. It has been suggested before by numerical simulations; see section 8.6.1 of [6], where it is referred to as “catastrophic grazing-sliding.” It has since been observed in a model of a superconducting resonator [15], which to our knowledge is the first time it has been identified in experiments.

By inspection, sections 5.1–5.3 exhaust the possible sliding bifurcations of orbits in the unfolding given by (5.4). Reversing the arrow of time reverses the stability of sliding but, up to time direction, all cases are equivalent to the three described above.

5.4. Sliding Bifurcation at an Invisible Fold. Consider the system given by taking $h(x) = x_2 - \frac{1}{2}x_1^2$ from (4.1) with the straightened vector field of (3.1). By result (2) of Definition 2.1 this describes an invisible fold. We treat this similarly to the visible fold, again setting $\rho = x_3$ in (5.1). Hence, we find that an unfolding of the *sliding bifurcation at an invisible fold* is given by $\psi = 0$, where

$$(5.6) \quad \begin{aligned} \psi(x) &= x_3 - x_2 + h(x)\Theta[-h(x)] \quad \text{and} \\ h(x) &= x_2 - \frac{1}{2}x_1^2. \end{aligned}$$

This is shown in Figure 5.1(iv). We will now describe this figure.

The sliding region on $h = 0$ is in $x_1 > 0$, and sliding segments flow away from the fold. Orbits impact the manifold on the curve $x_0(\mu) = (\mu, \frac{1}{2}\mu^2, \frac{1}{2}\mu^2)$, and we can label orbits by μ . Every orbit near an invisible fold must cross the manifold and hence has an impact coordinate. At $\mu = 0$ a nongeneric orbit hits the fold, implying a sliding bifurcation. This orbit hits the manifold transversally from $h < 0$, then slides. For $\mu > 0$, orbits impact the manifold from below and then slide. For $\mu < 0$, orbits cross the manifold into $h > 0$, then impact again at $x_1 = -\mu$ and slide. See Figure A.1(3) for the illustration of this at a flat switching manifold. It describes, for example, switching-sliding of a limit cycle as shown in Figure 1.3(iii).

The case with unstable sliding is found by reversing time in (3.1), but by inspection, up to time reversal, no sliding bifurcations other than Figure 5.1(iv) are possible. So far we have shown that three of the known sliding bifurcations (grazing-sliding, crossing-sliding, and switching-sliding in Figure 1.3) and a new one (catastrophic grazing-sliding) take place at a fold. In the next section we show that the only other previously known sliding bifurcation, adding-sliding in Figure 1.3(iv), takes place at a cusp.

5.5. Sliding Bifurcation at a Visible Cusp. Now consider the vector field in (3.1) with the switching manifold $h(x) = x_2 + \frac{1}{3}x_1^3 + x_3x_1 = 0$ from (4.2). By Definition 2.2, this has a cusp at the origin. From (5.1), the unfolding is the surface $\psi = 0$, where

$$(5.7) \quad \begin{aligned} \psi(x) &= \rho(x_3) - x_2 + h(x)\Theta[-h(x)] \quad \text{and} \\ h(x) &= x_2 + \frac{1}{3}x_1^3 + x_3x_1, \end{aligned}$$

as shown in Figure 5.2. Solving (5.2), we find that the impact coordinates satisfy $\rho(x_3) = x_2 = -\frac{1}{3}x_1^3 - x_3x_1$. Hence, we can parameterize the impact coordinates as

$$(5.8) \quad x_0(\mu_1, \mu_2) = (\mu_1, -\frac{1}{3}\mu_1^3 - \mu_1\mu_2, \mu_2).$$

Since x_3 is constant along the flow, substituting $\rho = -\frac{1}{3}\mu_1^3 - \mu_1\mu_2$ into (5.7) gives

$$(5.9) \quad \psi(x) = \frac{1}{3}(x_1 - \mu_1)(x_1^2 + x_1\mu_1 + \mu_1^2 + 3\mu_2) - h(x)\Theta[h(x)].$$

Because this requires two parameters, μ_1 and μ_2 , an orbit at the cusp has a two-parameter unfolding. This means that a one-parameter family of orbits does not generically intersect the cusp directly from $h > 0$ or $h < 0$.

Curves of fold points branch from the origin: a visible fold along $x = x_0(\sqrt{-\mu_2}, \mu_2)$ and an invisible fold along $x = x_0(-\sqrt{-\mu_2}, \mu_2)$, for $\mu_2 < 0$. The separatrix between sliding and crossing dynamics is the surface $\psi_{sl} = 0$ whose impact coordinates lie along a visible fold, where $\mu_1 = \sqrt{-\mu_2}$, which is therefore given by

$$(5.10) \quad \psi_{sl} = \frac{1}{3}(x_1 - \sqrt{-\mu_2})^2(x_1 + 2\sqrt{-\mu_2}) - h(x)\Theta[h(x)].$$

As shown in Figure 5.2, orbits in a stable sliding region flow toward the visible fold, then escape the switching manifold within the sliding separatrix. By Definition 2.2 there are two cases to consider. The system in (3.1) gives an invisible cusp, since $(\mathcal{L}_{f^+}^3 h)(\mathcal{L}_f h) > 0$. This has sliding segments only for $\mu_2 < 0$ (or $x_3 < 0$, $h = 0$) and is shown in Figure 5.2(i). Furthermore, the sliding segment tangent to the cusp consists of only a single point, and therefore cannot give rise to sliding bifurcations.

If we reverse the time direction in $h > 0$ of (3.1) so that $(\mathcal{L}_{f^+}^3 h)(\mathcal{L}_f h) < 0$, we obtain the visible cusp as shown in Figure 5.2(ii). In this case there is a nongeneric

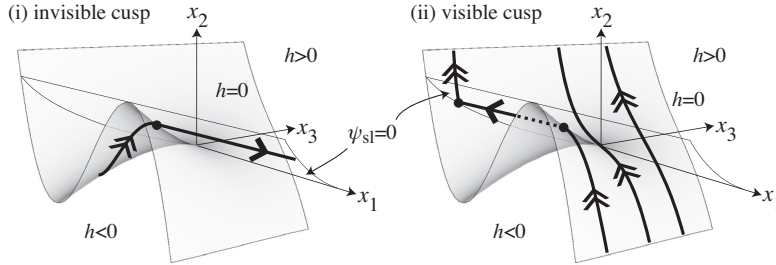


Fig. 5.2 The cusp, with switching manifold $h = x_2 + \frac{1}{3}x_1^3 + x_3x_1 = 0$ and sliding separatrix $\psi_{sl} = 0$ given by (5.10). Sliding segments are shown with double arrows. (i) At the invisible cusp the sliding region is $h = 0$, $x_3 < -x_1^2$. (ii) At the visible cusp the sliding region is $h = 0$, $x_3 > -x_1^2$. The vector field in $h < 0$ is vertically upward for stable sliding; reverse arrows for unstable sliding.

sliding segment with a visible tangency to the sliding boundary at the cusp (recall Figure 1.2(iii) for the definition of a visible tangency). This means that a one-parameter sliding bifurcation can occur, and its unfolding is given by the separatrix $\psi_{sl} = 0$ combined with sliding segments on $h = 0$. Since (5.10) has only one parameter, μ_2 , it defines a one-parameter unfolding for the *sliding bifurcation at a visible cusp*.

Reversing the overall time direction, we obtain visible and invisible cusps with unstable sliding. The phase portraits are the same as the stable cases up to time direction, so the only distinct one-parameter sliding bifurcation at a cusp is the visible case, shown in Figure 5.2(ii). This is illustrated at a flat switching manifold in Figure A.1(4). An example of it is adding-sliding of a limit cycle, as shown in Figure 1.3.

By considering the map $(\mu_1, \mu_2) \mapsto x_0(\mu_1, \mu_2)$ from (5.8), we can obtain the bifurcation diagram for sliding bifurcations near a cusp as shown in Figure 5.3. Sliding bifurcations at a fold take place at the visible fold (V) or the invisible fold (I), and degenerate combinations occur at the cusp. The separatrix from (5.10) impacts the switching manifold along the curve $\mu_2 = -\mu_1^2/4$ (R).

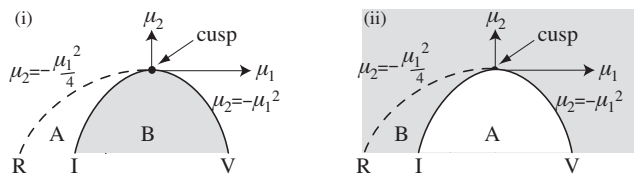


Fig. 5.3 Bifurcation curves in parameter space (μ_1, μ_2) for (i) the invisible cusp and (ii) the visible cusp. Visible (V) and invisible (I) fold branches separate sliding (shaded) and crossing (unshaded). Grazing orbits impact along R. The flow in $h > 0$ maps points from region A to B.

If we return to (5.7), we can obtain a typical unfolding by letting $\rho(x_3) = \rho_1 + \rho_2 x_3$, where ρ_1 and ρ_2 are constants that, respectively, specify the height and angle, with respect to the switching manifold, of a family of orbits parameterized by x_3 . Such a surface has four topologically different forms, depending on the signs of the quantities ρ_1 and $\rho_1 - \frac{1}{3}\rho_2^3$: the unfolding contains one visible grazing orbit if $\rho_1 < 0$, one invisible

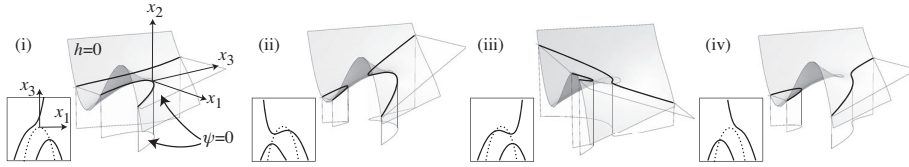


Fig. 5.4 The family of unfoldings from (5.7) with (i) $\rho_1 > 0$ and $\rho_1 - \rho_2^3/3 > 0$, (ii) $\rho_1 > 0$ and $\rho_1 - \rho_2^3/3 < 0$, (iii) $\rho_1 < 0$ and $\rho_1 - \rho_2^3/3 > 0$, and (iv) $\rho_1 < 0$ and $\rho_1 - \rho_2^3/3 < 0$. The intersections $h = \psi = 0$ are depicted inset and have turning points along the folds (dotted).

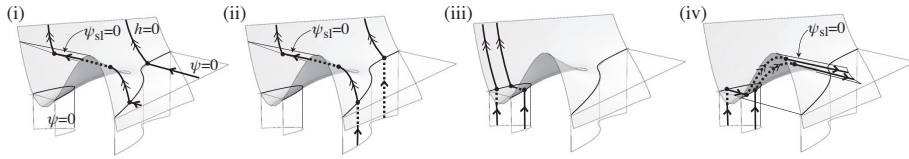


Fig. 5.5 An example of the unfoldings from (5.7) with $\rho_1 < 0$ and $\rho_1 < \rho_2^3/3$. (i)–(iii) show a visible cusp, and (iv) shows an invisible cusp. These exhibit sliding bifurcations: (i)–(ii) at a visible cusp (from Figure 5.2(ii)), and (iii)–(iv) at an invisible fold (from Figure 5.1(iv)). Sliding orbits escape on the separatrix $\psi_{sl} = 0$. Stable sliding cases are shown; simply reverse arrows for unstable sliding.

grazing orbit if $\rho_1 > 0$, and three grazing orbits in total if $\rho_1(\rho_1 - \frac{1}{3}\rho_2^3) < 0$. These are shown in Figure 5.4. They unfold the generic series of sliding bifurcations that will be observed by one-parameter variation of an orbit near a cusp, including all possible sliding bifurcations at the folds.

An example of a one-parameter unfolding is given in Figure 5.5, showing the same surface unfolding orbits around a cusp whether it is visible (i)–(iii) or invisible (iv).

5.6. Catastrophic Sliding Bifurcations at a Two-Fold. Up to now we have seen four sliding bifurcations in which an orbit changes continuously, but nondifferentiably, and one catastrophic case where the orbit changes discontinuously. In this section we show that there are three further sliding bifurcations that are catastrophic in nature, hitherto unclassified, and all originating from the two-fold.

Consider the vector field in (3.1), with the switching manifold $h(x) = x_3 + \frac{1}{2}\alpha x_1^2 - \frac{1}{2}\beta x_2^2 + x_1 x_2 = 0$ from (4.3). If the Hessian determinant over x_1, x_2 , given by $(\partial^2 h / \partial x_1^2)(\partial^2 h / \partial x_2^2) - (\partial^2 h / \partial x_1 \partial x_2)^2 = -(1 + \alpha\beta)$, is negative, then the manifold is a saddle; if it is positive, then the manifold is a bowl (similar to Figure 5.7).

Because the two-fold consists of tangencies to both sides of the manifold, the constant g in (5.3) is 1. Hence, by (5.1), the unfolding $\psi = 0$ is given by

$$(5.11) \quad \begin{aligned} \psi(x) &= \rho(x_3) - x_3 \quad \text{and} \\ h(x) &= x_3 + \frac{1}{2}\alpha x_1^2 - \frac{1}{2}\beta x_2^2 + x_1 x_2. \end{aligned}$$

By (5.2), impact coordinates satisfy $\rho(x_3) = x_3 = -\frac{1}{2}\alpha x_1^2 + \frac{1}{2}\beta x_2^2 - x_1 x_2$ and can be parameterized as

$$(5.12) \quad x_0(\mu_1, \mu_2) = (\mu_1, \mu_2, -\frac{1}{2}\alpha\mu_1^2 + \frac{1}{2}\beta\mu_2^2 - \mu_1\mu_2).$$

The folds lie along $\mathcal{L}_f^+ h = \alpha\mu_1 + \mu_2 = 0$ and $\mathcal{L}_f^- h = \mu_1 - \beta\mu_2 = 0$, with the signs of the second derivatives $\mathcal{L}_{f^+}^2 h = \alpha$ and $\mathcal{L}_{f^-}^2 h = -\beta$, respectively, determining whether

they are visible or invisible. At a visible fold, orbits escape the switching manifold and form sliding separatrices. By solving $\psi = 0$ so that its impact coordinates lie along a fold, we find that the sliding separatrices are given by $\psi_{sl} = 0$, where

$$(5.13) \quad \psi_{sl} = -x_3 + \frac{1 + \alpha\beta}{2\alpha\beta} \begin{cases} \beta x_2^2 & \text{if } h \geq 0, \\ -\alpha x_1^2 & \text{if } h \leq 0. \end{cases}$$

An orbit will not generically hit the two-fold from $h > 0$ or $h < 0$, since this requires that both of the parameters μ_1 and μ_2 vanish. Similarly to the cusp, to find sliding bifurcations we must consider sliding segments.

Without analyzing the sliding vector field f^{sl} in detail, we can use its boundary conditions, (1.4), to infer what forms are topologically possible. These conditions state that the sliding vector field f^{sl} , at a point along a fold, is equal to whichever of f^+ or f^- is tangent to the switching manifold at that point. Thus, $f^{sl} = f^+$ where $\mathcal{L}_{f^+}h = \alpha x_1 + x_2 = 0$, and $f^{sl} = f^-$ where $\mathcal{L}_{f^-}h = x_1 - \beta x_2 = 0$. This implies that f^{sl} points outwards from the stable sliding region at a visible fold and inwards at an invisible fold. (It does the opposite in the unstable sliding region.) Then only the sliding topologies shown in Figure 5.6 are possible. It is a straightforward exercise to verify this by calculating the sliding vector field explicitly using (1.3). These have been listed before [10, 15, 30], but not considered to be the source of sliding bifurcations aside from for remarks made in [14].

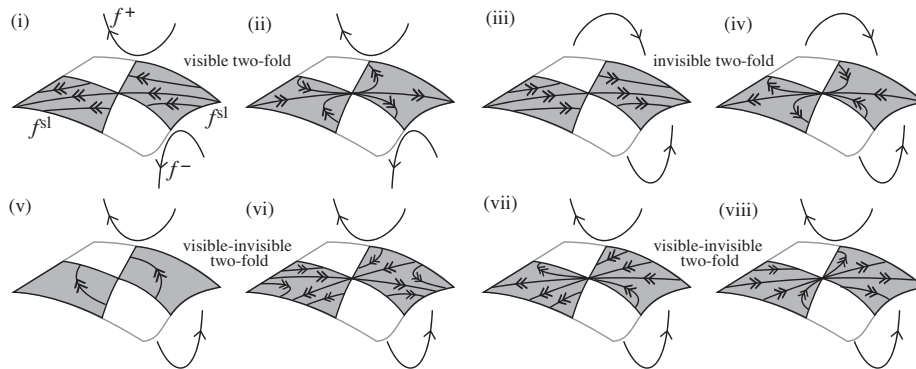


Fig. 5.6 The sliding vector field topologies at the two-folds. Shading regions are shaded. There are two topologies at a visible two-fold (i)–(ii), where $\alpha, \beta < 0$, two at an invisible two-fold (iii)–(iv), where $\alpha, \beta < 0$, and four at a visible-invisible two-fold (v)–(viii), where $\alpha\beta < 0$.

Only the cases in Figures 5.6(i), (vi), and (vii) give rise to one-parameter sliding bifurcations. These are the only cases in which not only does a sliding segment hit the two-fold, but its intersection with the switching manifold changes under perturbation as well. (In Figure 5.6(v) no sliding segments hit the two-fold; in the remaining cases any sliding bifurcations are trivial by Definition 1.3.) The unfoldings are illustrated in Figure 5.7, found by combining sliding trajectories with the sliding separatrices from (5.13).

Figure 5.7(i) depicts the *sliding bifurcation at a visible two-fold*. This occurs when $\alpha, \beta > 0$, in which case the Hessian determinant of h over x_1, x_2 is $-(1 + \alpha\beta) < 0$, so the switching manifold is a saddle. If the sliding vector field has the form of

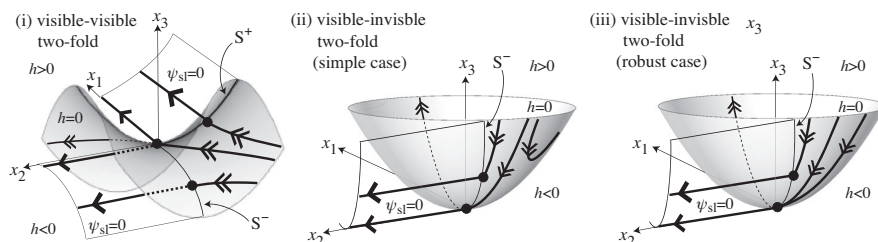


Fig. 5.7 Catastrophic sliding bifurcations at a two-fold for (i) the visible two-fold (ii) the visible-invisible two-fold (simple case); and (iii) the visible-invisible two-fold (robust case). The stable and unstable sliding regions are bounded by folds marked S^+ , where $\alpha x_1 + x_2 = 0$, and S^- , where $x_1 - \beta x_2 = 0$, at which orbits escape and form the separatrices $\psi_{sl} = 0$ given by (5.13). At the two-fold singularity the solutions are nonunique, producing orbits that enter the unstable sliding region (canards) and orbits that escape the manifold.

Figure 5.6(i), then a nongeneric sliding segment intersects the two-fold. At the two-fold singularity itself the dynamics is nonunique, since both boundary conditions in (1.4) apply there and are contradictory. Thus, an orbit may escape into $h > 0$ or $h < 0$ or enter the unstable sliding region as shown. Depending on which way we perturb the nongeneric orbit, we find that an orbit escapes the manifold into either $h > 0$ or $h < 0$ on the sliding separatrix ψ_{sl} given by (5.13).

Figures 5.7(ii)–(iii) depict the two cases of the *sliding bifurcation at a visible-invisible two-fold*. These can occur if $\alpha\beta < 0$. The switching manifold can be either a saddle or bowl depending on the sign of the Hessian determinant of h ; the figure shows bowls with $-1 - \alpha\beta > 0$. In both cases, a nongeneric sliding segment intersects the two-fold. At the two-fold point the dynamics is nonunique, since orbits can either escape the manifold or enter the unstable sliding region. Perturbing the nongeneric orbit in one direction gives a sliding segment that intersects the visible fold and escapes $h = 0$ along the sliding separatrix. Perturbing in the opposite direction leads to two possible scenarios. Given the vector field from Figure 5.6(vi), the orbit will remain locally on the manifold, as shown in Figure 5.7(ii). We call this the *simple case*. Alternatively, given the vector field from Figure 5.6(vii), there is a one-parameter family of orbits that intersects the two-fold, as shown in Figure 5.7(iii). Here the intersection with the singularity persists and we call this the *robust case*.

Sliding orbits that pass through the two-fold point are “canards” as defined in [27]—trajectories that pass from stable to unstable invariant manifolds (sliding regions). In Figures 5.7(i)–(ii), the only canard is the nongeneric orbit, while in Figure 5.7(iii) there is a one-parameter family of canards, hence the “singular” and “robust” classification.

In the neighborhood of an invisible two-fold, given by $\alpha < 0$ and $\beta < 0$, orbits map repeatedly back onto the switching manifold. This case is interesting in its own right and has been extensively studied in [10, 13, 29]. The unfoldings $\psi = 0$, given by (5.11), form invariant surfaces around which orbits rotate until they impact and slide. These are associated with local bifurcations studied in [16], but the invisible two-fold does not produce any sliding bifurcations.

5.7. Completeness of the Classification. A general switching manifold may contain any number of the singularities we have studied. Their genericity, however,

Table 5.1 *The eight one-parameter sliding bifurcations. The catastrophic cases are 5–8.*

Sliding bifurcation	Figure
1. at a visible fold, grazing case	Figure 5.1(i)
2. at a visible fold, crossing case	Figure 5.1(ii)
3. at an invisible fold	Figure 5.1(iv)
4. at a visible cusp	Figure 5.2(ii)
5. at a visible fold, catastrophic case	Figure 5.1(iii)
6. at a visible two-fold	Figure 5.7(i)
7. at a visible-invisible two-fold, simple case	Figure 5.7(ii)
8. at a visible-invisible two-fold, robust case	Figure 5.7(iii)

means that when any singularity is perturbed it will degenerate into folds. The sliding bifurcations are generic in the sense that any system can be perturbed to one exhibiting only those bifurcations listed in Table 5.1.

To prove that this classification is complete is a rather straightforward exercise. We consider what singularities will generically be hit (intersected) by orbits, either individually or in one-parameter families. Recall from Definition 1.1 that a generic orbit is a concatenation of generic trajectories of (1.2) and of (1.3), and that a singularity is a point where, without loss of generality, $\mathcal{L}_{f+}h = h = 0$. Then we have the following lemma:

LEMMA 5.1. *If an orbit of (1.2)–(1.3) in \mathbb{R}^n , for $n \geq 2$, hits a singularity, the singularity is generically a fold.*

Proof. This is an immediate consequence of the fact that orbits can generically contain sliding segments, which are one-dimensional curves on the switching manifold, and the fold is the only codimension one singularity of $h = 0$, provided that, at the singularity, $\mathcal{L}_{f+}^2 h(x^*) \neq 0$ and $\mathcal{L}_{f-} h(x^*) \neq 0$ (see Definition 2.1). \square

LEMMA 5.2. *If a one-parameter family of orbits of (1.2)–(1.3) in \mathbb{R}^n , for $n \geq 3$, hits a singularity, the singularity is generically a fold, a cusp, or a two-fold.*

Proof. From Lemma 5.1, an orbit with a sliding segment may generically hit a fold, but will miss singularities of higher codimension. However, the intersection of a one-parameter family of orbits with a fold is a one-dimensional curve. Since a cusp or two-fold occurs at an isolated codimension one set in the locus of folds, it can occur generically along such a one-dimensional intersection and hence be hit by a one-parameter family of orbits. Now consider a higher codimension singularity. This is a codimension r set in a locus of folds with $r > 1$, and therefore does not occur generically in the one-dimensional intersection between a fold and a one-parameter family of orbits. This result is independent of the number of dimensions provided that $n \geq 3$, so the fold, cusp, and two-fold occur generically and therefore the lemma holds in \mathbb{R}^n for $n \geq 3$. \square

We therefore have the central result of this paper, repeated from section 1.

THEOREM 1.4 *A generic one-parameter sliding bifurcation in \mathbb{R}^n for any $n \geq 3$ is a sliding bifurcation at a fold, a cusp, or a two-fold.*

Proof. A generic one-parameter sliding bifurcation takes place at a tangency between the vector field and the switching manifold, which corresponds to a singularity where $\mathcal{L}_{f+}h = h = 0$. Its unfolding is a one-parameter family of orbits, which, by Lemma 5.2, may generically hit a fold, a cusp, or a two-fold, but not a higher codimension singularity. \square

If the derivatives that define a fold, cusp, or two-fold vanish, but the nondegeneracy conditions given in Definitions 2.1–2.3 are violated, then the singularity they

define has a higher codimension. Higher codimension singularities can be derived from section 4 with V taking the form of swallowtail and butterfly catastrophe manifolds [24], or by taking intersections of folds with cusps/two-folds, and so on. Lemma 5.2 implies that for an orbit to hit these, at least two parameters are required. We discuss these parameters briefly in the next section.

5.8. Two-Parameter Sliding Bifurcations. Surfaces $\psi = 0$ of the form given by (5.1) can also be used to describe unfoldings of higher codimension sliding bifurcations. Consider the cusp or two-fold. An orbit that hits the cusp from $h > 0$ or $h < 0$ has the form $0 = \frac{1}{3}x_1^3 + h\Theta[h]$, $x_3 = 0$ (see (5.7)). By varying the two parameters μ_1 and μ_2 , we obtain a two-parameter unfolding. This codimension two scenario has been described in [17] for a visible or invisible cusp with stable sliding. Similarly, an orbit that hits the two-fold from $h > 0$ or $h < 0$ can be reached only by control of two parameters in the unfolding from (5.11). This has not been considered before in the literature on sliding bifurcations. By varying x_3 and either μ_1 or μ_2 , we obtain a two-parameter unfolding.

Also among the two-parameter sliding bifurcations are cases where a sliding segment intersects a codimension three singularity. We can refer to singularity theory, as in section 4, to find that for the piecewise-straightened vector fields in (3.1), the switching manifold $h = 0$ can take the form of the swallowtail $h = x_2 + (\frac{1}{4}x_1^4 + \frac{1}{2}x_3x_1^2 + x_4x_1)$, the lips $h = x_2 + (\frac{1}{3}x_1^3 + (x_3^2 + x_4)x_1)$ or beak-to-beak $h = x_2 + (\frac{1}{3}x_1^3 - (x_3^2 + x_4)x_1)$, and the fold-cusp $h = x_4 + (\frac{1}{3}x_1^3 + x_3x_1 + \frac{1}{2}x_2^2)$, where “ $\pm\frac{1}{2}x_2^2$ ” is a Morse term similar to that which describes a fold.

In every case, two-parameter sliding bifurcations take place at singularities that arise as subsets along the locus of folds, cusps, and two-folds. They are therefore comprised of degenerate combinations of the eight one-parameter sliding bifurcations introduced in section 5.

6. Concluding Remarks. By considering a piecewise-straight vector field with a curved switching manifold, we have studied the geometry that gives rise to sliding bifurcations. We have thus found that eight sliding bifurcations can occur as one parameter is varied in a generic Filippov system. They can be divided into two types: the regular sliding bifurcations 1–4 in Table 5.1, in which an orbit changes continuously and remains unique, and the catastrophic sliding bifurcations 5–8 in Table 5.1, in which an orbit changes discontinuously and is nonunique at the bifurcation itself.

This paper aims to provide a foothold for a bifurcation theory of piecewise-smooth systems that is as yet in its infancy. We have singled out the geometry of discontinuity induced bifurcations in sliding systems, focusing on the singularities and bifurcations that arise through loss of transversality between a vector field and a switching manifold. To these fundamentals we must add bifurcations on switching manifolds that have self-intersections or corners, and bifurcations of equilibria or invariant manifolds. The study of these for dimension $n > 2$ has barely begun.

It is worth reemphasizing that sliding bifurcations are *global* bifurcations (see Figure 1.4). They affect global sets (limit cycles, stable manifolds, etc.) that graze the switching manifold, but the bifurcation relies only on the geometry in the neighborhood of grazing. Global conditions give orbits in the unfolding a specific identity. A sliding bifurcation can be viewed locally as a bifurcation of orbits with no actual bifurcation of the underlying vector field.

The catastrophic sliding bifurcations are characterized as perturbations of orbits that impact a boundary of unstable sliding. Interpreted as the piecewise-smooth limit of a regularized vector field [31], the nonuniqueness of solutions at the bifurcation can

be interpreted as a cascade of orbits that penetrate the unstable sliding region. Far from being a pathological result of nonsmoothness, they are a common feature of real world models. They occur in singular perturbation problems such as the van der Pol system with relation to canards and relaxation oscillations [5, 12, 18], where the sliding vector field is comparable to the “reduced” (or slow) subsystem. They have also been proposed as the mechanism for sudden temperature oscillations observed in superconducting resonators [15, 25], and have been shown to be generic in switched feedback controllers [4].

A truly pathological feature of Filippov systems is the nondeterminism faced where both vector fields are tangent to the switching manifold (the two-fold, fold-cusp, etc.). This presents an ongoing dilemma for the interpretation of piecewise-smooth models, particularly since, in the sliding bifurcation at a visible-invisible two-fold (see Figure 5.7(ii)), a limit cycle can jump instantly from sliding to robust nondeterministic behavior. The resolution is likely to lie in closer study of the sliding bifurcations at two-folds in models of real world systems.

Appendix. Normal Forms at a Flat Switching Manifold. Given the piecewise-constant vector field in (3.1) and normal forms for singularities of the switching manifold in section 4, we now find coordinates in which the switching manifold is flat (and the vector field is no longer straight). These are more common in the literature on piecewise-smooth systems, and therefore useful for illustration.

Given a manifold written locally in the form $h(x) = x_i + V(x)$ as in (4.1)–(4.3), we make the smooth transformation to coordinates $y = (y_1, y_2, y_3)$ in which the switching manifold is given by $y_i = 0$. The unfolding function (5.1) is then given by $\psi(y) = \rho(y_3) + V(y) - y_i g(y)$. We now demonstrate the transformation for each of the singularities in Definitions 2.1–2.3.

Near the fold, as described in section 5.1, a transformation to $(y_1, y_2, y_3) = (x_1, h, x_3)$ gives

$$(A.1) \quad (\dot{y}_1, \dot{y}_2, \dot{y}_3) = \begin{cases} (1, \pm y_1, 0) & \text{if } y_2 > 0, \\ (0, 1, 0) & \text{if } y_2 < 0. \end{cases}$$

Sliding bifurcations at a fold in these coordinates are shown in parts 1, 2, 3, and 5 of Figures A.1.

Near the cusp in section 5.5, a transformation to $(y_1, y_2, y_3) = (x_1, h, x_3)$ gives

$$(A.2) \quad (\dot{y}_1, \dot{y}_2, \dot{y}_3) = \begin{cases} (1, y_1^2 + y_3, 0) & \text{if } y_2 > 0, \\ (0, 1, 0) & \text{if } y_2 < 0. \end{cases}$$

The sliding bifurcation at a visible cusp is shown in part 4 of Figure A.1.

Near the two-fold in section 5.6, we transform to $(y_1, y_2, y_3) = (x_1, x_2, \gamma h)$, where γ is a scaling constant that can take different values either side of the switching manifold. A similar constant at the fold or cusp has no topological effect, but at the two-fold it must be included for the sliding vector field to realize all of the topologies in Figure 5.6. Without loss of generality, we can let $\gamma = 1$ for $h > 0$ and let $\gamma = \gamma^-$ for $h < 0$. Then the two-fold vector field near a flat switching manifold is given by

$$(A.3) \quad (\dot{y}_1, \dot{y}_2, \dot{y}_3) = \begin{cases} (1, 0, \alpha y_1 + y_2) & \text{if } y_3 > 0, \\ (0, 1, (y_1 - \beta y_2)\gamma^-) & \text{if } y_3 < 0. \end{cases}$$

The sliding bifurcations at a two-fold then are shown in parts 6–8 of Figure A.1.

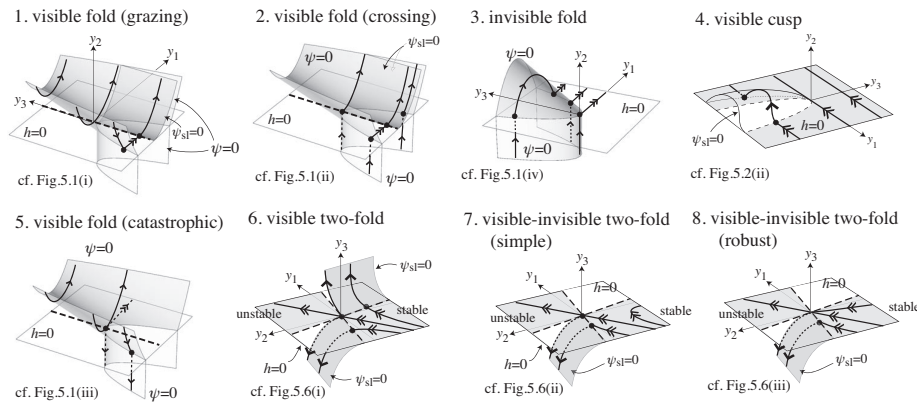


Fig. A.1 The eight generic one-parameter sliding bifurcations, shown in coordinates where the switching manifold $h = 0$ is flat. The labels 1–8 correspond to the classification in Table 5.1. The surface $\psi = 0$ is the unfolding. Sliding segments are shown with double arrows, and leave $h = 0$ on the sliding separatrix $\psi_{sl} = 0$.

The piecewise-smooth vector fields in (A.1)–(A.3) are equivalent to normal forms defined by previous authors, up to coordinate transformations that are linear in $h > 0$ and $h < 0$ and continuous at $h = 0$. The fold, cusp, and two-folds all appear in the seminal work by Filippov [10], with local vector fields similar to (A.1)–(A.3). Normal forms have since been derived for each of these. The cusp follows directly from the cusp at the boundary of a manifold given in [26]. Teixeira’s normal forms for two-folds [29, 30] are obtained from (A.3) by letting $(x, y, z) = (y_1 + \alpha^{-1}y_2, (y_1 - \beta y_2)\gamma^-, y_3)$, then f^+ is written in [29, 30] as $X(x, y, z) = (1, \gamma^-, x)$ and f^- as $Y(x, y, z) = (\alpha^{-1}, -\beta\gamma^-, y)$, in terms of the parameters α, β, γ^- (this excludes Teixeira’s case “a5,” where the vector fields are not everywhere transverse).

The cusp is also equivalent to the codimension one “double tangency” studied in planar Filippov systems in [20]. There, a parameter (called α) replaces the coordinate y_3 in (A.3) (which is valid since $\dot{y}_3 = 0$). The two-folds are referred to as “collisions of tangencies,” but in this case the vector fields are not equivalent, since the two-fold requires at least three dimensions to express generically.

Acknowledgments. The authors wish to thank D. Chillingworth for many helpful discussions and J. Guckenheimer and P. Holmes for comments on earlier drafts of this work.

REFERENCES

- [1] M. E. BROUCKE, C. PUGH, AND S. SIMIC, *Structural stability of piecewise smooth systems*, Comput. Appl. Math., 20 (2001), pp. 51–90.
- [2] J. W. BRUCE AND P. J. GIBLIN, *Curves and Singularities*, Cambridge University Press, Cambridge, UK, 1984.
- [3] D. R. J. CHILLINGWORTH, *Differential Topology with a View to Applications*, Pitman, London, 1976.
- [4] A. COLOMBO, M. DI BERNARDO, E. FOSSAS, AND M. R. JEFFREY, *Teixeira singularities in 3D switched feedback control systems*, Systems Control Lett., 59 (2010), pp. 615–622.
- [5] M. DESROCHES, B. KRAUSKOPF, AND H. M. OSINGA, *Mixed-mode oscillations and slow manifolds in the self-coupled Fitzhugh-Nagumo system*, Chaos, 18 (2008), article 015107.

- [6] M. DI BERNARDO, C. J. BUDD, A. R. CHAMPNEYS, AND P. KOWALCZYK, *Piecewise-Smooth Dynamical Systems: Theory and Applications*, Springer, London, 2008.
- [7] M. DI BERNARDO, F. GAROFALO, L. GLIELMO, AND F. VASCA, *Switchings, bifurcations, and chaos in DC/DC converters*, IEEE Trans. Circuits Syst. I, 45 (1998), pp. 133–141.
- [8] M. DI BERNARDO, P. KOWALCZYK, AND A. NORDMARK, *Bifurcations of dynamical systems with sliding: Derivation of normal-form mappings*, Phys. D, 170 (2002), pp. 175–205.
- [9] M. I. FEIGIN, *Forced Oscillations in Systems with Discontinuous Nonlinearities*, Nauka, Moscow, 1994 (in Russian).
- [10] A. F. FILIPPOV, *Differential Equations with Discontinuous Righthand Sides*, Kluwer Academic, Dordrecht, The Netherlands, 1998.
- [11] M. GOLUBITSKY AND D. G. SCHAEFFER, *Singularities and Groups in Bifurcation Theory*, Appl. Math. Sci. 51, Springer, New York, 1984.
- [12] J. GUCKENHEIMER, K. HOFFMAN, AND W. WECKESSER, *The forced van der Pol equation I: The slow flow and its bifurcations*, SIAM J. Appl. Dyn. Syst., 2 (2003), pp. 1–35.
- [13] E. A. JACKSON, *Perspectives of Nonlinear Dynamics*, Vol. 1, Cambridge University Press, Cambridge, UK, 2009.
- [14] M. R. JEFFREY, *Two-folds in nonsmooth dynamical systems*, in Proceedings of the 2nd IFAC Conference on Analysis and Control of Chaotic Systems, IFAC-PapersOnLine, 2009; available online from www.ifac-papersonline.net/Detailed/42846.html.
- [15] M. R. JEFFREY, A. R. CHAMPNEYS, M. DI BERNARDO, AND S. W. SHAW, *Catastrophic sliding bifurcations and onset of oscillations in a superconducting resonator*, Phys. Rev. E, 81 (2010), article 016213.
- [16] M. R. JEFFREY AND A. COLOMBO, *The two-fold singularity of discontinuous vector fields*, SIAM J. Appl. Dyn. Syst., 8 (2009), pp. 624–640.
- [17] P. KOWALCZYK AND M. DI BERNARDO, *Two parameter degenerate sliding bifurcations in Filippov systems*, Phys. D, 204 (2005), pp. 204–229.
- [18] M. KRUPA AND P. SZMOLYAN, *Relaxation oscillation and canard explosion*, J. Differential Equations, 174 (2001), pp. 312–368.
- [19] Y. A. KUZNETSOV, *Elements of Applied Bifurcation Theory*, 2nd ed., Springer, New York, 1998.
- [20] YU. A. KUZNETSOV, S. RINALDI, AND A. GRAGNANI, *One-parameter bifurcations in planar Filippov systems*, Internat. J. Bifur. Chaos Appl. Sci. Engrg., 13 (2003), pp. 2157–2188.
- [21] R. I. LEINE AND N. HENK, *Dynamics and Bifurcations of Non-smooth Mechanical Systems*, Springer, Berlin, 2004.
- [22] S. MANCINI, M. A. S. RUAS, AND M. A. TEIXEIRA, *On divergent diagrams of finite codimension*, Cadernos de Matematica, 1 (2000), pp. 179–194.
- [23] J. PALIS AND W. DE MELO, *Geometric Theory of Dynamical Systems*, Springer, Berlin, 1982.
- [24] T. POSTON AND I. N. STEWART, *Catastrophe Theory and Its Applications*, Dover, Mineola, NY, 1996.
- [25] E. SEGEV, B. ABDO, O. SHTEMLUCK, AND E. BUKS, *Novel self-sustained modulation in superconducting stripline resonators*, Europhys. Lett., 78 (2007), article 57002.
- [26] J. SOTOMAYOR AND M. A. TEIXEIRA, *Vector fields near the boundary of a 3-manifold*, in Dynamical Systems (Valparaiso, 1986), R. Bamon, R. Labarca, and J. Palis, eds., Lecture Notes in Math. 1331, Springer, Berlin, 1988, pp. 169–195.
- [27] P. SZMOLYAN AND M. WECHSELBERGER, *Canards in \mathbb{R}^3* , J. Differential Equations, 177 (2001), pp. 419–453.
- [28] M. A. TEIXEIRA, *On topological stability of divergent diagrams of folds*, Math. Z., 180 (1982), pp. 361–371.
- [29] M. A. TEIXEIRA, *Stability conditions for discontinuous vector fields*, J. Differential Equations, 88 (1990), pp. 15–29.
- [30] M. A. TEIXEIRA, *Generic bifurcation of sliding vector fields*, J. Math. Anal. Appl., 176 (1993), pp. 436–457.
- [31] M. A. TEIXEIRA, J. LLIBRE, AND P. R. DA SILVA, *Regularization of discontinuous vector fields on \mathbb{R}^3 via singular perturbation*, J. Dynam. Differential Equations, 19 (2007), pp. 309–331.
- [32] V. I. UTKIN, *Variable structure systems with sliding modes*, IEEE Trans. Automat. Control, 22 (1977), pp. 212–222.
- [33] S. M. VISHIK, *Vector fields near the boundary of a manifold*, Vestnik Moskov. Univ. Ser. I Mat. Meh., 27 (1972), pp. 13–19.
- [34] Z. T. ZHUSUBALYEV AND E. MOSEKILDE, *Bifurcations and Chaos in Piecewise-Smooth Dynamical Systems*, World Scientific, River Edge, NJ, 2003.